ELSEVIER

Journal of Neuroscience Methods xxx (2006) xxx–xxx

JOURNAL OF NEUROSCIENCE METHODS

www.elsevier.com/locate/jneumeth

Large-scale neural ensemble recording in the brains of freely behaving mice

Longnian Lin [a,b], Guifen Chen [b], Kun Xie [a], Kimberly A. Zaia [b,1], Shuqing Zhang [b], Joe Z. Tsien [a,b,*]

[a] *Shanghai Institute of Brain Functional Genomics, The Key laboratories of MOE and SSTC, East China Normal University, Shanghai 200062, China*
[b] *Center for Systems Neurobiology, Departments of Pharmacology and Biomedical Engineering, Boston University, Boston, MA 02118, USA*

Received 18 October 2005; received in revised form 24 November 2005; accepted 20 December 2005

Abstract

With the availability of sophisticated genetic techniques, the mouse is a valuable mammalian model to study the molecular and cellular basis of cognitive behaviors. However, the small size of mice makes it difficult for a systematic investigation of activity patterns of neural networks in vivo. Here we report the development and construction of a high-density ensemble recording array with up to 128-recording channels that can be formatted as single electrodes, stereotrodes, or tetrodes. This high-density recording array is capable of recording from hundreds of individual neurons simultaneously in the hippocampus of the freely behaving mice. This large-scale in vivo ensemble recording techniques, once coupled with mouse genetics, should be valuable to the study of complex relationship between the genes, neural network, and cognitive behaviors.

Keywords: Ensemble recording; Microdrive; Stereotrode; Tetrode; Hippocampus; Memory; Startle; In vivo recording; CA1 region; Mouse

1. Introduction

The arrival of functional genomics era is marked by the ever-increasing need to investigate physiological functions of genes in vivo. As approximately 60–70% of the genes have been estimated to be either brain-specific or highly enriched in the brain, it is important to study the gene function in cognitive behaviors. The rapid development of a series of inducible and region-specific gene knockout (Mack et al., 2001; Shimizu et al., 2000; Tsien et al., 1996a) or more recently, inducible protein knockout techniques (Wang et al., 2003), as well as transgenic methods (Hedou and Mansuy, 2003; Kida et al., 2002) have permitted precise investigations of the relationship between genes and behaviors. For example, series of conditional gene knockout experiments have allowed us to show that the knockout of the NMDA receptor in the CA1 region of the hippocampus impairs the CA1 synaptic plasticity and leads to profound memory deficits (Tsien et al., 1996b). Moreover, genetic enhancement of NMDA receptor coincidence-detection function through the up-regulation of the NR2B subunit in the mouse forebrain can lead to significant enhancement in both learning and memory (Tang et al., 1999; Wong et al., 2002), thereby stringently validating the Hebb's learning rule (Tsien, 2000). Thus, various mouse genetic techniques provide powerful ways to dissect the molecular and genetic mechanisms of cognition in the mammalian species.

One crucial link in our understanding of the relationship between genes and behaviors lies at our ability to measure neural network properties and dynamical patterns associated with genetic and behavioral changes. Over the past several decades, neuroscientists have obtained valuable insights by using EEG to map global brain responses or by recording the activity of one or a few neurons at a time. However, neither approach provides a direct means to investigate the network mechanisms underlying information processing. Encouragingly, in recent years, simultaneous monitoring of activities of many neurons has become more feasible in rats (Gray et al., 1995; Harris et al., 2000; McNaughton et al., 1983; Schmidt, 1999). Since mice are typically only about one tenth to one fifteenth of the body weight of rats (20–30 g versus 300–450 g of body weight), many of the ensemble recording microdrives designed for rats are often too big to be used for the recording in mice. A mouse version

* Corresponding author. Center for Systems Neurobiology, Department of Pharmacology School of Medicine, Department of Biomedical Engineering College of Engineering, Boston University, Building L-601, 715 Albany Street, Boston, MA 02118, USA. Tel.: +1 617 414 2655; fax: +1 617 414 2658.
E-mail address: jtsien@bu.edu (J.Z. Tsien).
[1] Current address: Stanford University Neuroscience Graduate Program.

0165-0270/$ – see front matter © 2006 Elsevier B.V. All rights reserved.
doi:10.1016/j.jneumeth.2005.12.032

of such microdrives has been reported to be able to carry up to 24-channels that can simultaneously record approximately 20–30 individual neurons in the brains of freely behaving mice (McHugh et al., 1996). Here we report the design and construction of a high-density microdrive system which can hold up to 128-channels and allows for a measurement of activities of over two hundreds individual neurons in the brains of freely behaving mice. This high-density ensemble recording array should be a valuable tool in the study of relationships between the genes, neural network, and behaviors.

2. Methods

2.1. Construction of 96-channel recording microdrive

We set out to design a recording microdrive which would allow us to record neural activity from a large number of individual CA1 cells in the hippocampus. The 96- or 128-channel electrodes consist of two-independently movable bundles of 32 stereotrodes or 16 tetrodes (64-channel on each side of the hippocampi). The foundation for the microdrive was prepared from three or four 36-pin connector arrays positioned in parallel; one array was secured with epoxy glue (5 min epoxy system, ITW Performance Polymers, Riviera Beach, FL) to both sides of the microdrive base, and the third (and fourth for 128 channel headstage) array was separated from the middle array with a rectangular plastic spacer (Fig. 1A and B). A bundle of 16 pieces of polyimide tubing (TSP 075150: inner diameter 75 um, outer diameter 150 um, Polymicro technologies, Phoenix, AX) was glued to each of the two-independently movable screw nuts on the microdrive base. After the glue had dried, polyimide was trimmed to ensure that at least 1–2 mm of tubing would protrude from either end of the microdrive base throughout the advancing range of the microdrive (Fig. 1B).

Each stereotrode or tetrode was constructed by twisting a folded piece of two or four wires (STABLOHM 675, H-FORMVAR, 25 μm for stereotrode and 13 μm for tetrode, California Fine Wire), securing the two strands together with a low intensity heat source, and removing the insulation from the tips of the free ends over an open flame. Each completed stereotrode or tetrode was threaded through one of the polyimide tubes secured to the microdrive screw nuts. After all electrode had been inserted into separate polyimide tubes, the twisted ends of the wires were cut to a length that extended 3–4 mm beyond the end of the polyimide bundle, and the wires were then secured to the polyimide tubing with glue.

The free end of each stereotrode or tetrode (insulation had been removed) were wrapped around adjacent connect pins (Fig. 1C). In addition, each wrapped connector pin was individually coated with silver paint to enhance conduction (Silver Print II, GC Electronics). A reference wire (magnet wire, 0.01 mm^2, Belden electronic division) was soldered to the four pins on ends of each connector array. In the final stages of microdrive construction, the looped stereotrode were secured to the foundation of the microdrive (Fig. 1D) to reduce the potential for accidental damage following surgery. In addition, the tips of the tetrode were plated with gold (Cyanida Gold solution, SIFCO Selective plating) to a final impedance of 500–800 kΩ. The silver-coated connector pin arrays were then coated with nail enamel (Chanel, Inc., New York) for insulation.

2.2. Surgical procedure

Wild-type B6BCA/J mice were given continuous access to food and water in their cages. Mice were handled for several days prior to surgery to minimize the potential stress of human interaction. On the day of surgery, the mouse was anesthetized with i.p. injection of 60 mg/kg ketamine (Bedford Laboratories, OH) and 4 mg/kg Dormitor (Pfizer Animal Health, NY). The mouse's head was immobilized in a stereotaxic frame and its eyes were coated with sterile ocular lubricant (Puralube Vet Ointment, Pharmaderm, Melville NY). After the hair above the

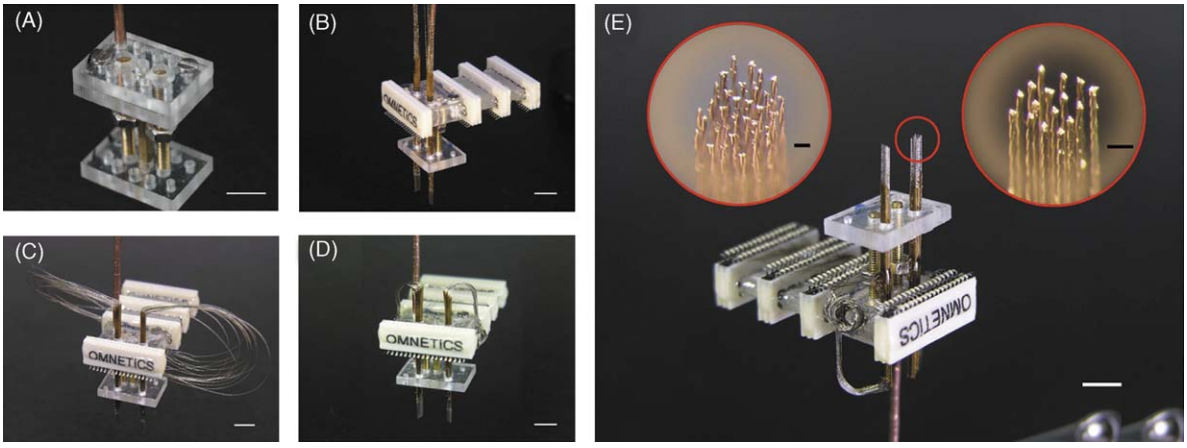

Fig. 1. Construction of the high-density ensemble recording microdrive. (A) The base foundation for the microdrive. (B) Four 36-pin connector arrays were positioned the base of the microdrive in parallel. Each bundle of 32 pieces (for stereotetrodes) or 16 pieces (for tetrodes) of polyimide tubing was glued to an independently movable screw nut on the microdrive base. (C) A microdrive on the assembly stage. The free ends of electrode wires are wrapped around to adjacent connect pins. (D) A fully assembled, adjustable 128-electrode microdrive. (E) One hundred and twenty eight-channels can be formatted with either tetrodes (right inset) or stereotrodes (left inset) on each bundle. The tip of the two electrode bundles was shaped at a certain angle (10°–20°) to fit the contour of the dorsal CA1 cell layer. Black scale bar in red circles of E are 100 μm. White scale bars in A–D are 3 mm.

skull had been removed, Betadine solution was applied to the skin surface, an incision was made along the midline of the skull. The edges of the cut skin were held to the sides with small clips, and the membranous layer was removed to expose the skull. Hydrogen peroxide was applied to the skull surface to permit visualization of the bregma position along the midline. The positions for the two bundles (2.0 mm lateral to bregma and 2.3 mm posterior to bregma on the both right and left sides) were then measured and marked. Four holes were drilled in a rectangular array surrounding the coordinates designed for the stereotrode or tetrode bundles, and small screws were secured in each of these holes and fixed with dental cement. Holes for the two stereotrode or tetrode bundles were then drilled and dura was removed carefully. The stereotaxic apparatus was then used to lower the stereotrode or tetrode bundles into these holes and into the mouse's cortex. The gaps surrounding the stereotrodes or tetrode were filled with softened paraffin and the microdrive was stabilized with dental cement. The reference wire attached to the two posterior head screws was soldered to the reference wire affixed to the connector pin arrays of the microdrive, and copper mesh was wrapped around the entire microdrive to protect the wires from potential damage. The mouse was then aroused with an injection of 2.5 mg/kg Antisedan and returned to its home cage.

2.3. *In vivo recording and spike sorting*

The mouse was allowed to recover for several days before advancing the electrodes. The connector pin arrays on the microdrive were first attached to pre-amplifiers with extended cables to allow for the monitoring of neuronal signals using the 128-channel Plexon system in stereotrode or tetrode format. A helium-filled mylar balloon was tied to the cables for alleviating the weight of the apparatus and cables, thereby enabling the mouse to move freely. Typically 4–5 days after surgery, we begin to advance the electrodes (the mice were gently hold still by hands). The stereotrode or tetrode bundles were advanced slowly toward the hippocampal CA1 region, in daily increments of about 0.07 mm until the tips of the electrodes had reached the CA1 as deduced from an assessment of field potential and neuronal activity patterns.

We subsequently recorded the ensemble activity of a large number of individual neurons during freely behaving states. The recorded spike activities from those neurons were processed in the manner as previously described (Lin et al., 2005): first, the spike waveforms and their associated time stamps for each of 128-channels were stored in data files using Plexon system format (*.plx). The artifact waveforms were removed and the spike waveform minima were aligned using the Offline Sorter 2.0 software (http://www.plexon.com, Dallas, TX) which resulted more tightly clustered waveforms in principal component space. The Plexon system data files (*.plx) were then converted to Neuralynx system format (*.nst) and spike-sorted with the MClust3.3 program (http://www.cbc.umn.edu/~redish/mclust, David Redish). This program permits classification of multidimensional continuous data. Its cluster splitting feature (Buzsaki lab) yields superior accuracy in comparison to the other available spike-sorting software and is therefore particularly suitable for spike sorting of hippocampal signals.

Principal component analysis was used to extract defining features from the spike wave shapes that are used as part of the input for the MClust3.3 spike sorting program. The first two principal components, as well as the peak height, valley value, FFT and total energy of spike waveform parameters were calculated for each channel, and units were identified and isolated in high-dimensional space through the use of an autoclustering method (KlustaKwik 1.5) (Harris et al., 2000). After autoclustering, the clusters containing non-spike waveforms were deleted using 'KlustaKwik Selection' function, and then the units were further isolated using a manual cluster cutting method in MClust. Only units with clear boundaries and less than 0.5% of spike intervals within a 1 ms refractory period are included in the present analysis. At the end of experiments, the mouse was anesthetized and a small amount of current was applied to four channels in the microdrive to mark the positioning of the electrode bundle.

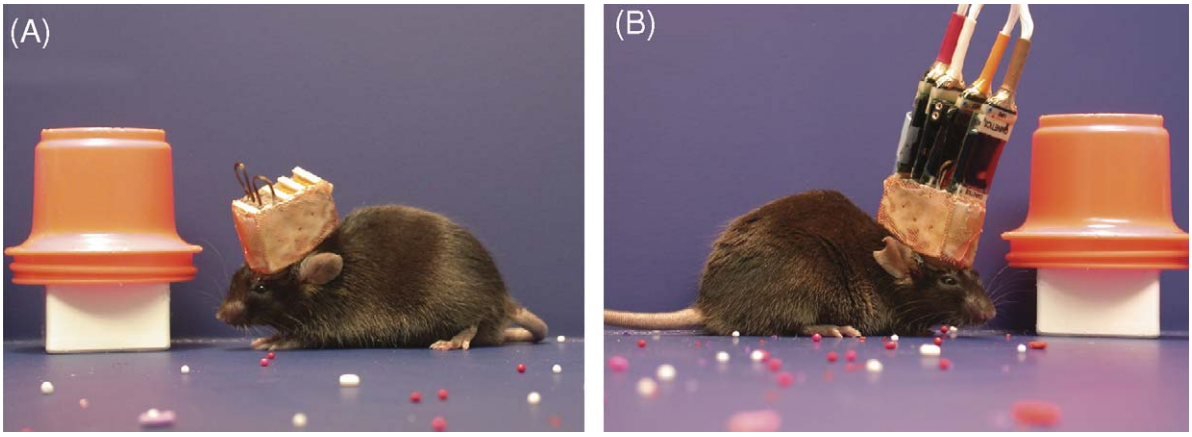

Fig. 2. High-density in vivo ensemble recording in freely behaving mice. (A) Here shows an example of a freely behaving mouse implanted with a completed 128-channel microdrive in bilateral hippocampi. (B) This ultra-light microdrive, even after connected to 128-channel headstages and cables, allows the mouse to move freely in various situations, such as running, exploring, eating, grooming, sleep and performing learning tasks, etc.

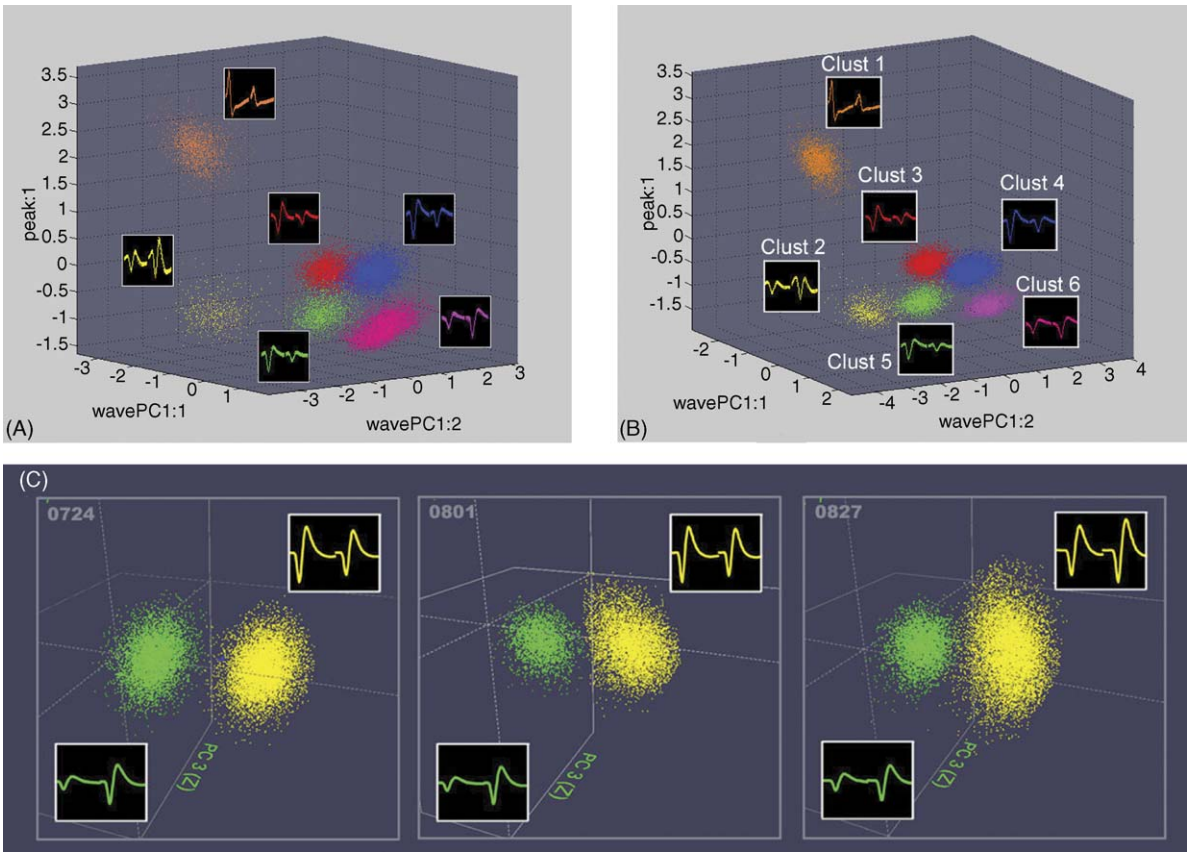

Fig. 3. Stable recordings of single units in mice. (A) Automatic spike sorting was performed using the KlustaKwik method and was followed by the MClust method for manual cluster cutting and merging. Six sorted units detected by a stereotrode are presented here in different colors. The stereotrode waveforms (the waveforms of each unit detected by each tip of the steretrode, shown side-by-side) of the individual units are shown along the corresponding clusters. (B) The panel shows the same six stable units at the completion of 6-h recording. (C) The panels show the same two single units recorded from a stereotrode remained stable for more than 1 month. The letters on the top left corner indicate the date of the recording, 24 July, 1 August, and 27 August. The insets at the bottom left corner and top right corner show the waveforms of the single units detected by two channels of the stereotrode.

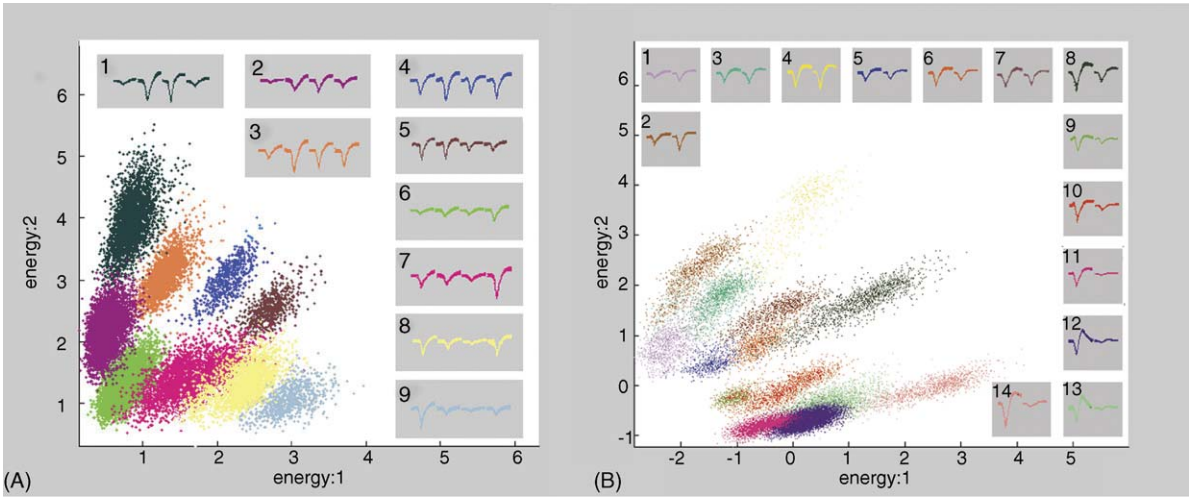

Fig. 4. Separation of multiple single units by either stereotrodes or tetrodes. (A) Nine single units were detected by a single tetrode. Average waveforms of nine separated units and the corresponding energy spike distributions were used for this classification. The insets show four waveforms side-by-side detected by the four channels of the tetrode. (B) Fourteen single units were detected by a single stereotrode. Average stereotrode waveforms of the putative separated units and the corresponding energy spike distributions were used for this classification. The insets show that two waveforms were detected by the two channels of the stereotrode.

Histological staining, with (1% cresyl echt violet) was used to confirm the electrode positions.

3. Results

3.1. Design and construction of high-density ensemble recording microdrive

We designed and constructed a high-density microdrive system that was specially adapted to the small size of mice. The electrode positions on the microdrive can be easily formatted according to the specific need for recording in various brain regions. Here we present the data gathered in the hippocampus as it is one of the regions known to be crucial for the formation of long-term memories (Sara, 2000; Scoville and Milner, 1957; Squire, 1987; Tsien et al., 1996b) and has been a major focus of systematic investigations which have produced extremely valuable insights into the molecular and neural mechanisms of learning-related behaviors (Disterhoft et al., 1986; Eichenbaum et al., 1999; Fenton and Muller, 1998; Leutgeb and Mizumori, 1999; O'Keefe and Nadal, 1978; Thompson, 2005; Wirth et al., 2003). Accordingly, we constructed an adjustable microdrive system that is suitable for recording on both sides of the hippocampus (with two adjustable bundles of totalling as many as 128-microelectrodes) (Fig. 1A and E). The distance between two bundles was based on the targeted recording sites on the dorsal hippocampus (2.0 mm lateral to bregma and 2.3 posterior to bregma on the both right and left sides). In addition, the ends of the 64 wires on each side were formatted at an angle (10°–20°) that would maximally follow the contour of CA1 pyramidal cell layer (Fig. 1E). An example of a freely behaving mouse implanted with such a high-density recording microdrive is shown in Fig. 2. This ultra-light microdrive allows the mouse to move freely in various situations, such as running, exploring, eating, grooming, sleep, performing learning tasks, etc. (Fig. 2).

The electrodes on our high-density microdrive can be formatted in the single electrode, stereotrode (two wires), or tetrode format (four wires). Therefore, the 128-channel recording electrodes can be formatted as either 32 tetrodes or 64 steretrodes corresponding to 32 or 64 recording sites, respectively (see top insets in Fig. 1E). Furthermore, our microdrive system can provide stable recordings in vivo as evident from the similar spike-sorting pattern obtained from the same electrode over 6 h (Fig. 3A and B), and in a few cases, even over 1 month (Fig. 3C). Both tetrodes and stereotrodes are capable of providing reliable separation of individual units (Fig. 4 and Table 1). On occasions, up to 14 stable units can be recorded and separated on a single steretrode (Fig. 4B). The quantitative measures of cluster quality in our spike-sorting were obtained by measuring the L-ratio and isolation distance (Mclust 3.3 software). These two measures, recently introduced by Schmitzr-Torbert et al., quantify how well separated the spikes of one cluster (putative unit) are from other spikes recorded simultaneously on the same multi-channel electrode (Schmitzer-Torbert et al., 2005). The good separation of units by our stereotrodes and tetrodes is evident from the measurements of L-ratio and isolation distance (Table 1).

Table 1
Reliable separation of single units

	L-ratio	Isolation distance (ID)
(A)		
Clust 1	0.0045	184.4
Clust 2	0.0005	118.7
Clust 3	0.0036	85.3
Clust 4	0.0062	79.5
Clust 5	0.0049	54.6
Clust 6	0.0155	218.4
Average	0.0058	123.5
(B)		
Clust 1	0.0247	30.1
Clust 2	0.0557	30.9
Clust 3	0.0049	12.8
Clust 4	0.0050	56.2
Clust 5	0.0799	39.9
Clust 6	0.2084	17.4
Clust 7	0.2428	9.9
Clust 8	0.0646	24.7
Clust 9	0.0235	68.6
Average	0.0788	32.3
(C)		
Clust 1	0.0764	25.9
Clust 2	0.0552	27.0
Clust 3	0.0518	26.9
Clust 4	0.0285	25.0
Clust 5	0.0563	23.0
Clust 6	0.0192	31.0
Clust 7	0.044	25.9
Clust 8	0.0141	33.1
Clust 9	0.0228	27.1
Clust 10	0.3007	15.7
Clust 11	0.0309	44.2
Clust 12	0.0526	24.6
Clust 13	1.9556	4.8
Clust 14	0.0449	37.0
Average	0.1966	26.5

(A) The L-ratio and isolation distance corresponding to the six clusters show in Fig. 3b provides quantitative measures for their separation quality. (B) The L-ratio and isolation distance corresponding to the nine clusters show in Fig. 4a provides quantitative measures for the tetrodes recording and separation. (C) The L-ratio and isolation distance corresponding to the fourteen clusters show in Fig. 4b provides quantitative measures for the stereotrodes recording and separation.

3.2. Activity patterns of CA1 single unit activity during running and sleep

It is known that the behavioral states of an animal are associated with different EEG patterns of the hippocampus. During locomotion and rapid eye movement (REM) sleep, the hippocampus generates characteristic theta rhythm (an EEG or an extracellular field recording signal oscillates in the approximately 4–12 Hz frequency range) (Alonso and Garcia-Austt, 1987; Buzsaki et al., 1985; Fox and Ranck, 1981; Ranck, 1973). Consistent with those reports, we observed that the hippocampus of freely behaving mice generated typical theta rhythm during running (Fig. 5A). Our simultaneous monitoring of theta activity and multiple single unit activity in the mouse hippocampus shows that some cells fire rhythmically in phase with theta

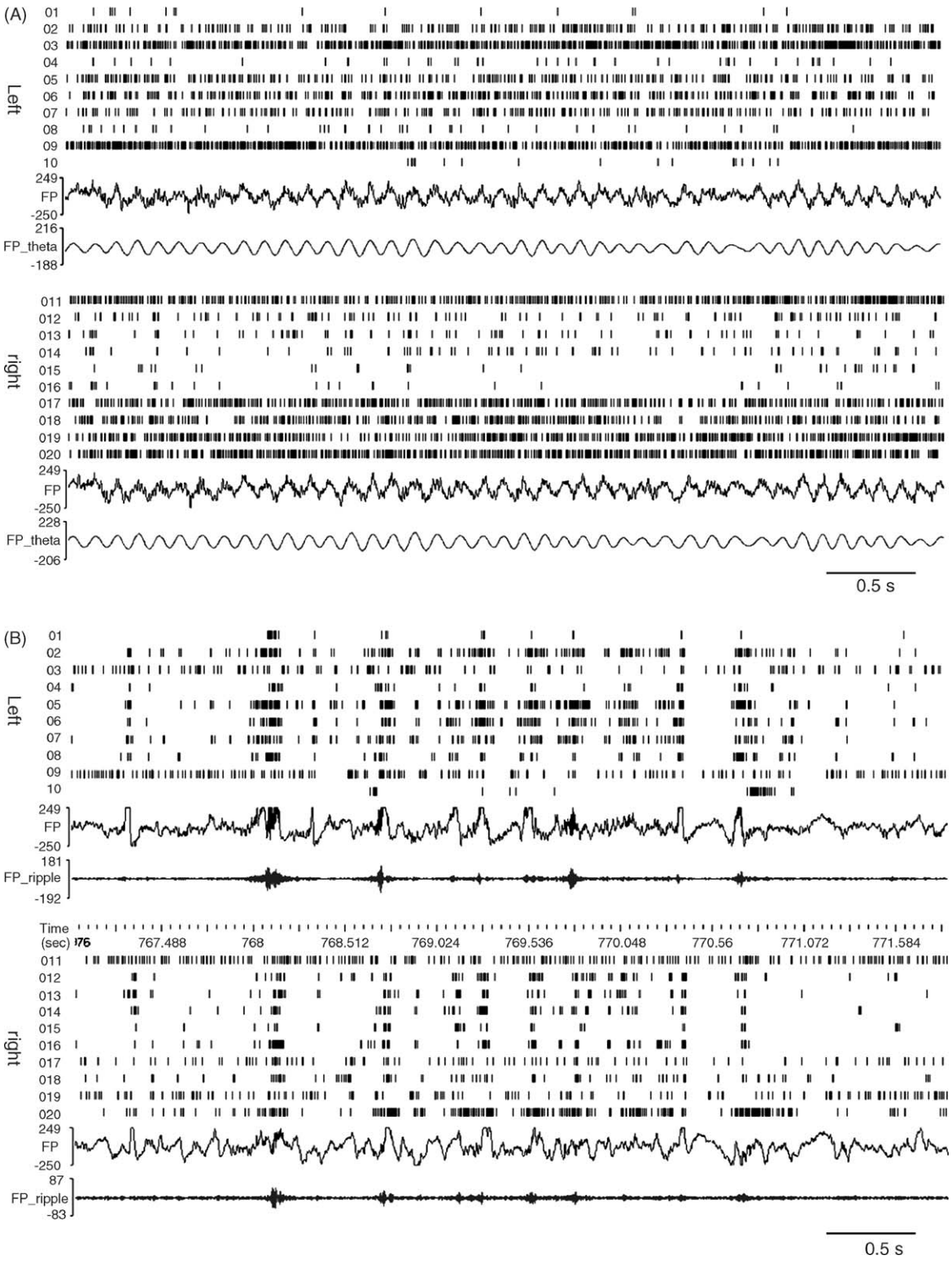

Fig. 5. Simultaneous recordings of large umbers of individual neurons in freely behaving mice. (A) The activity of the simultaneously recorded individual neurons from bilateral hippocampi in mice during locomotion (top two panels). Over 150 of the neurons were simultaneously recorded by the high-density ensemble array, and we selected 10 neurons from each side for illustration. The continuous strip chart (a total of 8 s) shows 10 individual neurons (#1–10) from the left hippocampus and 10 individual neurons (#11–20) from the right hippocampus during that time. Please note that the simultaneous field potential recording shows the typical theta rhythm oscillations (4–12 Hz) during running. (B) The activity of the simultaneously recorded individual neurons from bilateral hippocampi in mice during sleep. The simultaneous field potential recording shows the irregular waves as well as the ripple oscillations (150–250 Hz) during REM sleep. FP shows the original field potential recorded from the same channel with the spikes. *FP_theta* shows the field potential filtered with the 4–12 Hz spectrum from the original one, whereas *FP_ripple* shows the field potential filtered with the frequency range from 150 to 250 Hz from the original one.

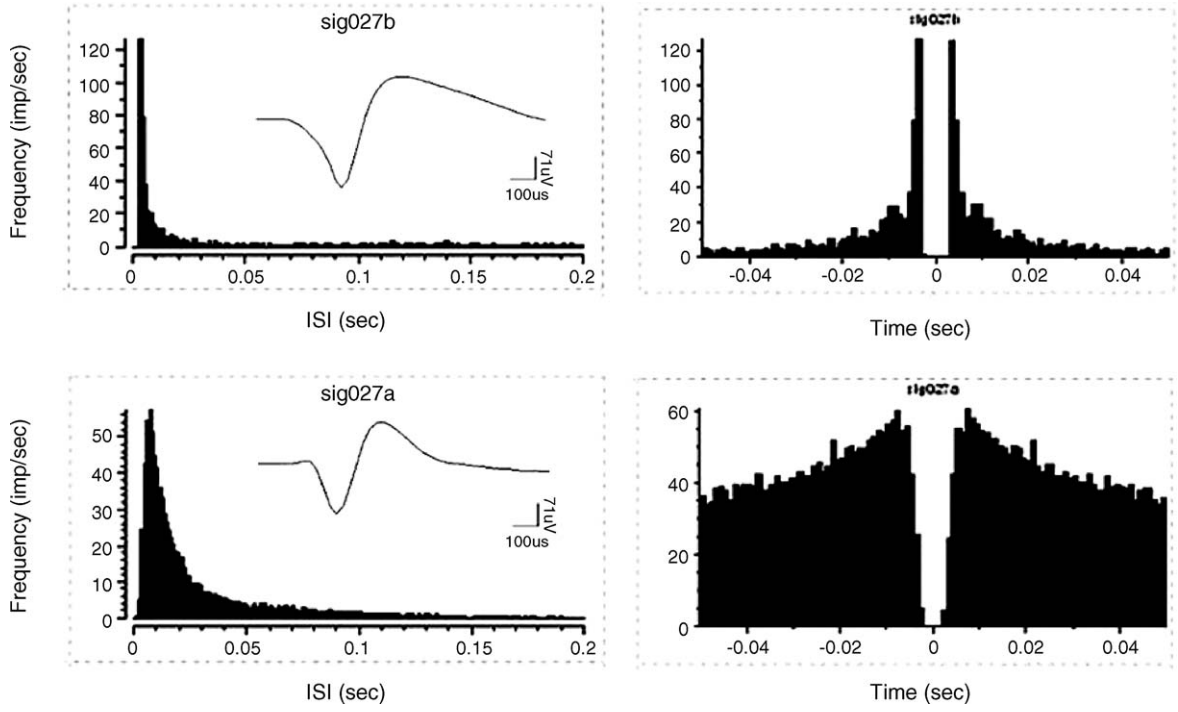

Fig. 6. Putative excitatory and inhibitory neurons. Discharge dynamics has characteristic difference between pyramidal cells and interneurons, reflected by their histograms (left side panels) and autocorrelograms of inter-spike intervals (right side panels). The putative pyramidal cell shown in the upper panels has lower mean firing rate and wider and more asymmetrical wideband waveform than the interneuron shown in the bottom panels. As known by the inter-spike-intervals plot, pyramidal cells have complex-spike bursts with 3–10 ms inter-spike intervals. Consequently, the autocorrelogram of pyramidal cells typically shows a characteristic peak at 3–5 ms, followed by a rapid exponential decay, whereas putative interneurons exhibited a much slower decay. The left panels show the histograms of inter-spike intervals. The *Y*-axes represent the frequency of the spike occurrence. This putative pyramidal cell exhibited typical burst firing, with the peak intraburst firing rate reaches 120 Hz, whereas the putative inhibitory cell had the mean firing rate at the 22 Hz. The insets within the left panels show waveforms. The right panels show the autocorrelograms of inter-spike intervals of these two cells.

waves, while other cells fire non-rhythmically. We also observed that during other behavioral states, such as immobile quiet awake state or non-REM sleep, the hippocampus produced irregular sharp waves (SPW) (Fig. 5B). It is believed that the sharp wave state during these behavioral states is due to the reduced release of neuromodulators by subcortical structures (Hasselmo and Schnell, 1994).

Consistent with previous studies in rats (Alonso and Garcia-Austt, 1987; Buzsaki et al., 1985; Fox and Ranck, 1981; Ranck, 1973), CA1 units in the mouse hippocampus can also be divided into two classes: principle units (putative pyramidal neurons) and theta units (putative interneurons), distinguishable by the width of the waveform, firing rates, and the inter-spike interval (Fig. 6). Putative pyramidal cells have low mean firing rates and have wider and asymmetrical wideband waveforms (top left insets of Fig. 6), whereas putative interneurons on average have higher discharge rates and narrower spike width (bottom left insets of Fig. 6). In addition, discharge dynamics of pyramidal cells and interneurons also differed as reflected by their autocorrelograms (the right insets in Fig. 6). Pyramidal cells are known to fire complex-spike bursts with 3–10 ms interspike intervals (Fox and Ranck, 1981; Harris et al., 2000; Ranck, 1973). Consequently, the autocorrelogram of pyramidal cells typically shows a characteristic peak at 3–5 ms, followed by a rapid exponential decay (top right inset in Fig. 6), whereas putative interneurons exhibits a much slower decay (bottom right inset in Fig. 6). In general, the number of pyramidal cells constitutes the majority of the recorded cells in the CA1 region.

3.3. Ensemble patterns of CA1 single unit activity in response to external stimuli

To further demonstrate that our high-density recording electrodes can monitor activity of many hippocampal CA1 neurons in response to learning-related episodic events, we delivered a sudden air blow to the back of the mouse. It has been reported that such natural stimuli can produce robust startling memories as measured by the place conditioning test (Lin et al., 2005). Indeed, we show that many neurons in the CA1 region exhibited changes in their firing frequency (Fig. 7). Those changes include transient increase, prolonged increase, transient decrease, and prolonged decrease of firing rates (Fig. 8). Thus, our results demonstrate that the high-density recording techniques are capable of large-scale monitoring of the activities of over hundreds of individual neurons in the hippocampus of freely behaving mice.

4. Discussion

The ability to monitor the real-time activity patterns of large numbers of individual neurons in freely behaving animals is crucial for our understanding how the brain encodes and processes cognitive information about the animal's behavioral

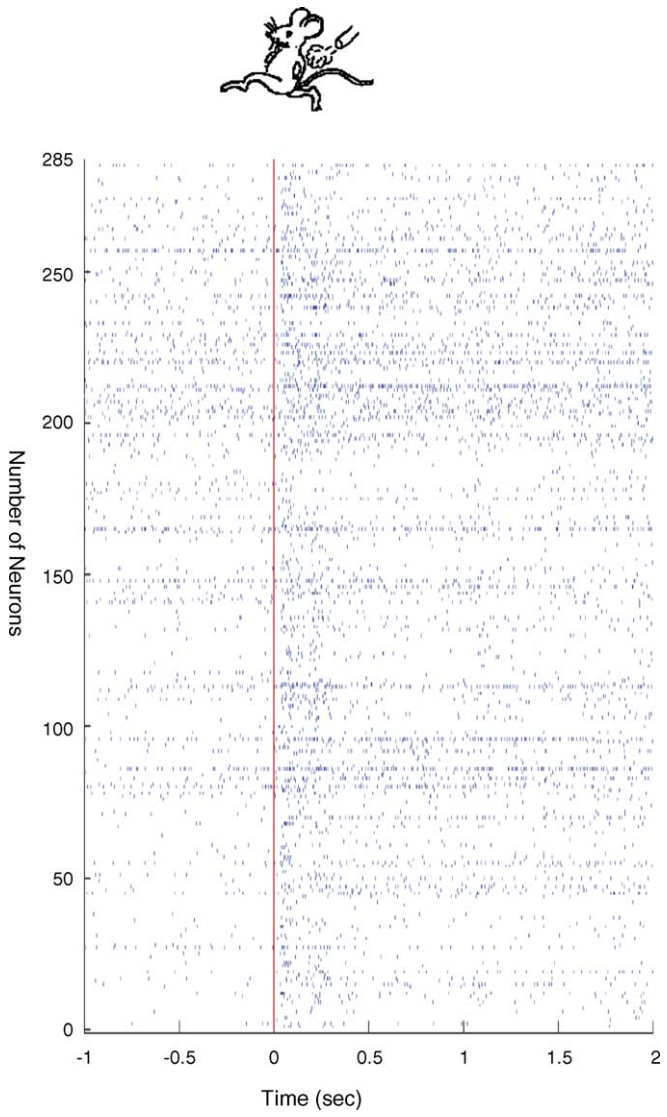

Fig. 7. Response of CA1 ensemble patterns to external stimuli. Robust changes in the firing patterns in CA1 neurons can be induced by startling stimuli such as the sudden air-blow delivered to the back of the mouse, illustrating the responsiveness of the neuronal population to external input. Here shows spike rasters of 260 simultaneously recorded single units from a mouse during a period of 1 s prior to and 2 s after the occurrence of single startling episodes of air-blow ($t = 0$ marked with vertical red line).

experiences. Over the past decade, the development and application of molecular biology and genetics have made mouse an ideal model organism to study the molecular and neural basis of cognitive behaviors. For example, it is now possible that a gene of interest can be knocked out in both a brain subregion-specific and temporally inducible manner (Shimizu et al., 2000; Tsien et al., 1996a). More recently, inducible protein knockout in mice has also been reported to further allow researchers to manipulate protein activities rapidly, with a temporal resolution at the timescale of minutes (Wang et al., 2003).

However, the network-level analysis of neural mechanisms of cognitive behaviors has lagged behind, largely due to the technical difficulties. The small size of a mouse, for example, has greatly constrained the numbers of individual neurons that researchers can record from using the traditional electrophysiological methods. With the recent technical advances, researchers have gained a great capacity for recording many neurons from various mammalian species, ranging from rats to cats to monkeys (Gray et al., 1995; Hoffman and McNaughton, 2002; McNaughton et al., 1983; Schmidt, 1999; Wills et al., 2005; Wilson and McNaughton, 1993). Here, we show that using our high-density recording arrays, the number of simultaneously recorded individual neurons in the mouse brain has increased from the traditional range of tens of cells to over two hundreds of individual cells.

Although the described design is currently made for recording in the mouse CA1 region, the basic construction can be easily customized and modified to fit the specific need for recording in other brain sites. Importantly, our microdrive system can be formatted in single, stereotrode, or tetrode format. While the tetrode format may offer the best separation of single units, the stereotrode format is still capable of achieving reliable separations of multi-units on most recording electrodes. On average, we can record and separate 5–7 units per steretrode (per site) in the hippocampus. This is highly consistent with the number of recorded units in the rat hippocampus using steretrodes as reported by others (Marta et al., 2003, 2004; McEchron et al., 2001; McNaughton et al., 1983). Thus, given the same number of channels available the tetrode format would lead to a 50% reduction in the numbers of recording sites in the CA1 region in comparison to the stereotrode format.

A major advantage of tetrode comes when the potentially recorded cells happen to be located with equal distance to the two recording channel tips of the steretrode and happen to exhibit the same waveform characteristics. Under this unique scenario, the steretrode would then have difficulty in discriminating them. By using two additional channels (relying on the differences in spatial location), a tetrode can differentiate between the waveforms of these "identical cells" (Gray et al., 1995; Harris et al., 2000). Based on our examinations of 99 single units measured by the tetrodes, as long as the amplitudes of the detected waveform by the two channels (stereotrode format) are sufficiently above the noise basal level, the stereotrodes can provide highly comparable isolation with 100% accuracy.

In addition, we have also assessed the second unusual scenario in which the recorded cells with the identical waveforms happen to be located in the middle-line "plane" of the two recording channel tips of the steretrode. We have calculated the occurrence probability of such cases where middle-line "plane" cells were unable to be resolved by steretrodes, as constituting only a tiny fraction (about 1.5% of our recordings in such cases, those ambiguous units were removed from further analysis). Although the vast majority of the recorded cells usually are not located on the middle-line "plane" between two recording tips of the steretrode (primarily because the CA1 pyramidal cell layer typically consists of only 2–3 rows), we did indeed observe those middle-line "plane" cells on some occasions. Fig. 9A shows all 10 clusters (single units) detected by a steretrode. There are six units clustered around the middle diagonal line (Fig. 9A). While it is still possible to distinguish them based on the subtle differences in peak amplitudes and wave shapes, in our practice

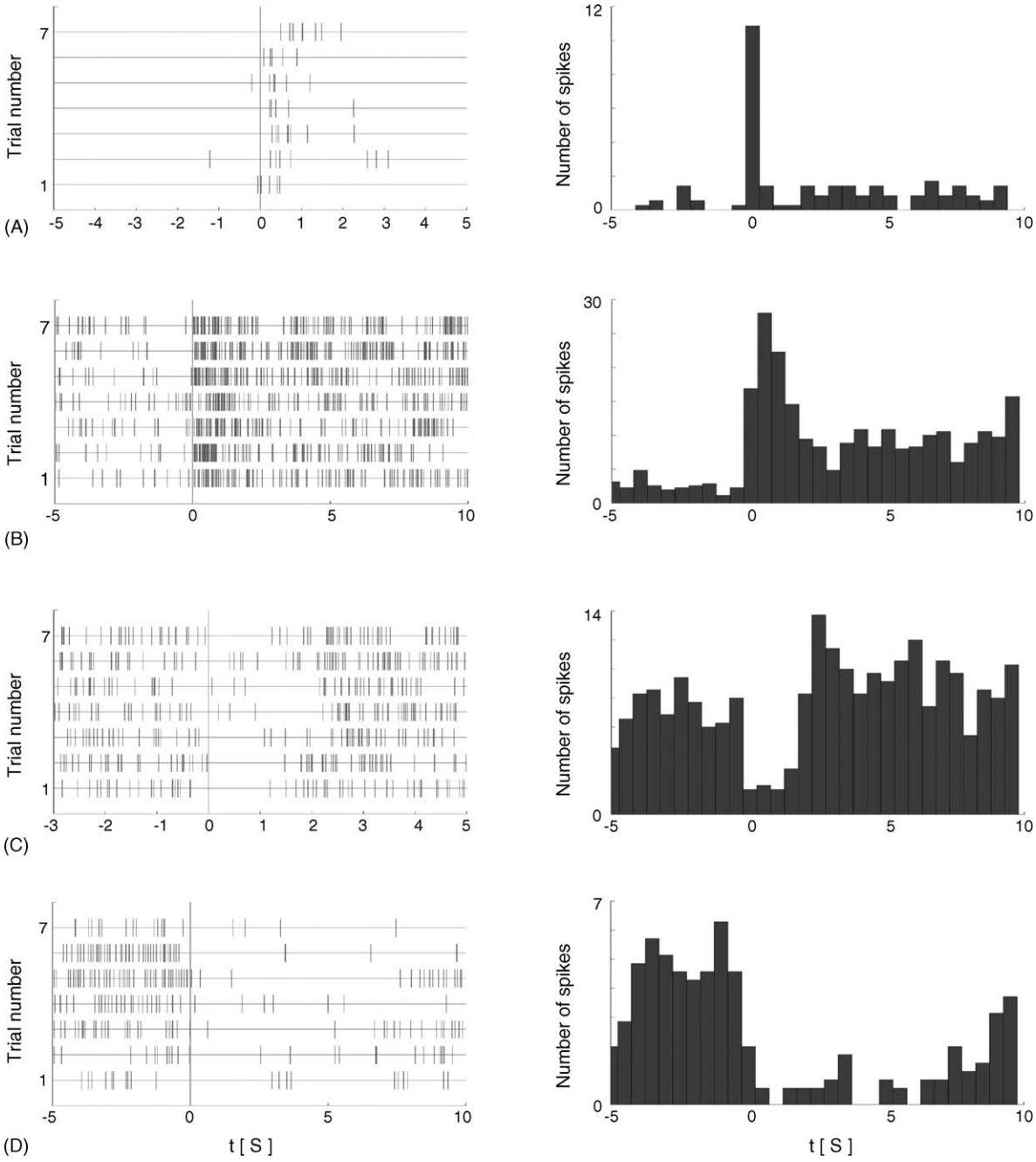

Fig. 8. Peri-event rasters and peri-event histograms of air-puff responsive cells in the CA1 region. Spike raster plots (left column, seven air-puff repetitions) and corresponding peri-event histogram (right, bin width 500 ms) for units exhibiting the four major types of firing changes observed: (A) transient increase, (B) prolonged increase, (C) transient decrease, and (D) prolonged decrease.

we simply discard them (Fig. 9B), thereby only selecting the four well-separated single units from this steretrode for further analysis. Therefore, using our above stringent criteria during the spike-sorting procedures, we can ensure all units used for subsequent data analysis are well separated with high confidence.

It is noteworthy that although our current microdrive is relatively lightweight, the connecting cable carrying 96 or 128 wires to the data acquisition systems can drastically increase the total weight, thereby restraining free movements of the animals. To solve this problem, we currently use a helium-filled mylar balloon tied to the cables for alleviating the weight of the apparatus and cables. This method is simple and efficient and enables the mouse to move freely during recording. In the near future, it might be desirable to further combine our microdrive system with a miniature telemetry system which can transmit signals via radio frequency in a wireless fashion. In deed, such a devise was recently reported (Chien and Jaw, 2005).

In conclusion, we report the design and construction of high-density ensemble recording arrays which allow the simultaneous recording of over two hundreds of individual neurons in the

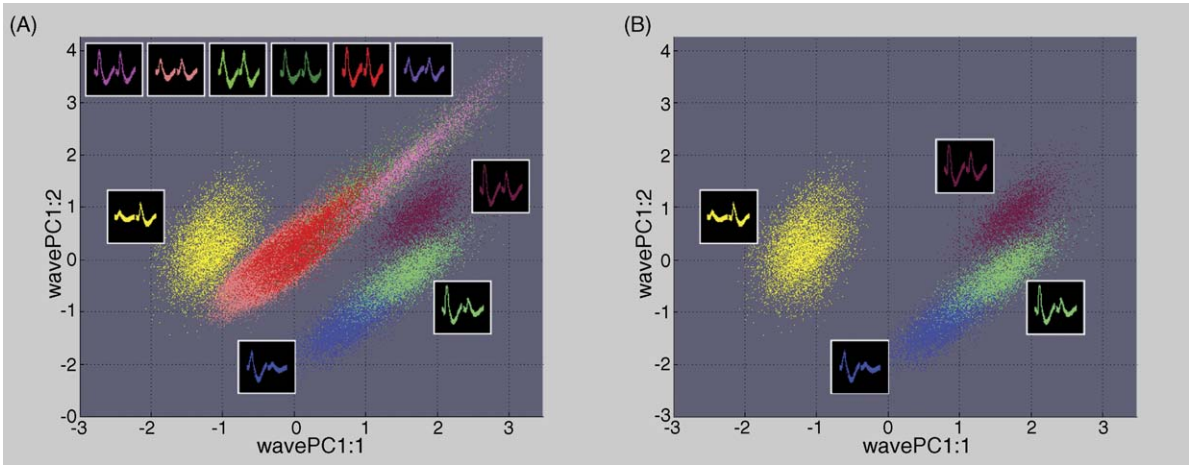

Fig. 9. Occurrence of middle-line "plane" cells during recording. (A) It shows all 10 clusters (single units) detected by a stereotrode. There are six units clustered around the middle diagonal line with the similar waveforms detected by both channels of the stereotrode (shown side by side in top insets). (B) Although it is possible to distinguish some of them based on the subtle differences in peak amplitudes and wave shapes, we simply discard them to ensure the quality of the spike sorting.

brain of freely behaving mice. It is conceivable that the combined application of genetic techniques with this large-scale in vivo recording technique should permit better study of complex relationship between the genes, neural network, and behaviors.

Acknowledgements

We thank Dr. Gyorgy Buszaki and his lab staff for discussion and advice on the design of the recording microdrive and other related technical issues. We also thank Dr. Remus Osan for discussion during the experiments and manuscript preparation. This research was supported by funds from NIMH, NIA, Burroughs Welcome Fund, ECNU Alumni Science Fund, and W.M. Keck Foundations (JZT), special funds for Major State Basic Research of China (NO2003CB716600), the key project of Chinese ministry of Education (NO104084), and Shanghai Science and Technology Commission (JZT and LL).

References

Alonso A, Garcia-Austt E. Neuronal sources of theta rhythm in the entorhinal cortex of the rat. Exp Brain Res 1987;67:493–501.

Buzsaki G, Rappelsberger P, Kellenyi L. Depth profiles of hippocampal rhythmic slow activity ('theta rhythm') depend on behaviour. Electroencephalogr Clin Neurophysiol 1985;61:77–88.

Chien C-N, Jaw F-S. Miniture telemetry system for the recording of action and field potentials. J Neurosci Methods 2005;147:68–73.

Disterhoft JF, et al. Conditioning-specific membrane changes of rabbit hippocampal neurons measured in vitro. Proc Natl Acad Sci USA 1986;83:2733–7.

Eichenbaum H, Dudchenko P, Wood E, Shapiro M, Tanila H. The hippocampus, memory, and place cells: is it spatial memory or a memory space? Neuron 1999;23:209–26.

Fox SE, Ranck Jr JB. Electrophysiological characteristics of hippocampal complex-spike cells and theta cells. Exp Brain Res 1981;41:399–410.

Fenton AA, Muller RU. Place cell discharge is extremely variable during individual passes of the rat through the firing field. Proc Natl Acad Sci USA 1998;95:3182–7.

Gray CM, Maldonado PE, Wilson M, McNaughton B. Tetrodes markedly improve the reliability and yield of multiple single-unit isolation from multi-unit recordings in cat striate cortex. J Neurosci Methods 1995;63:43–54.

Harris KD, Henze DA, Csicsvari J, Hirase H, Buzsaki G. Accuracy of tetrode spike separation as determined by simultaneous intracellular and extracellular measurements. J Neurophysiol 2000;84:401–14.

Hasselmo M, Schnell E. Laminar selectivity of the cholinergic suppression of synaptic transmission in rat hippocampal CA1. J Neurosci 1994;14:3898–914.

Hedou G, Mansuy IM. Inducible molecular switches for the study of long-term potentiation. Philos Trans R Soc Lond B Biol Sci 2003;358:797–804.

Hoffman KL, McNaughton BL. Coordinated reactivation of distributed memory traces in primate neocortex. Science 2002;297:2070–3.

Kida S, et al. CREB required for the stability of new and reactivated fear memories. Nat Neurosci 2002;5:48–55.

Leutgeb S, Mizumori SJY. Excitotoxic septal lesions result in spatial memory deficits and altered flexibility of hippocampal single-unit representations. J Neurosci 1999;19:6661–72.

Lin L, et al. Identification of network-level coding units for real-time representation of episodic experiences in the hippocampus. Proc Natl Acad Sci USA 2005;102:6125–30.

Mack V, et al. Conditional restoration of hippocampal synaptic potentiation in Glur-A-deficient mice. Science 2001;292:2501–4.

Marta AP, et al. Hippocampal place cells acquire location-specific responses to the conditioned stimulus during auditory fear conditioning. Neuron 2003;37:485–97.

Marta AP, et al. Putting fear in its place: remapping of hippocampal place cells during fear conditioning. J Neurosci 2004;24:7015–23.

McEchron, et al. Aging and learning-specific changes in single-neuron activity in CA1 hippocampus during rabbit trace eyeblink conditioning. J Neurophysiol 2001;86:1839–57.

McHugh TJ, Blum KI, Tsien JZ, Tonegawa S, Wilson MA. Impaired hippocampal representation of space in CA1-specific NMDAR1 knockout mice. Cell 1996;87:1339–49.

McNaughton BL, O'Keefe J, Barnes CA. The stereotrode: a new technique for simultaneous isolation of several single units in the central nervous system from multiple unit records. J Neurosci Methods 1983;8:391–7.

O'Keefe J, Nadal L. The hippocampus as a cognitive map. Oxford: Oxford University Press; 1978.

Ranck JB. Studies on single neurons in dorsal hippocampal formation and septum in unrestrained rats I. Behavioral correlates and firing repertoires. Exp Neurol 1973;41:461–531.

Sara SJ. Strengthening the shaky trace through retrieval. Nat Rev Neurosci 2000;1:212–3.

Schmidt EM. Electrodes for many single neuron recordings. In: Nicolels M, editor. Methods for neural ensemble recordings. CRC Press; 1999. p. 1–23.

Schmitzer-Torbert N, Jackson J, Henze D, Harris K, Redish AD. Quantitative measures of cluster quality for use in extracellular recordings. Neuroscience 2005;131:1–11.

Scoville WB, Milner B. Loss of recent memory after bilateral hippocampal lesions. J Neurol Neurosurg Psychiatr 1957;20:11–21.

Shimizu E, Tang YP, Rampon C, Tsien JZ. NMDA receptor-dependent synaptic reinforcement as a crucial process for memory consolidation. Science 2000;290:1170–4.

Squire LR. Memory and brain, 401. Oxford: Oxford University Press; 1987, 63–69.

Tang YP, et al. Genetic enhancement of learning and memory in mice. Nature 1999;401:630–69.

Thompson RF. In search of memory traces. Annu Rev Psychol 2005;56:1–23.

Tsien JZ. Building a brainier mouse. Sci Am 2000;282:62–8.

Tsien JZ, et al. Subregion- and cell type-restricted gene knockout in mouse brain. Cell 1996a;87:1317–26.

Tsien JZ, Huerta PT, Tonegawa S. The essential role of hippocampal CA1 NMDA receptor-dependent synaptic plasticity in spatial memory. Cell 1996b;87:1327–38.

Wang H, et al. Inducible protein knockout reveals temporal requirement of CaMKII reactivation for memory consolidation in the brain. Proc Natl Acad Sci USA 2003;10:4287–92.

Wills TJ, Lever C, Cacucci F, Burgess N, O'Keefe J. Attractor dynamics in the hippocampal representation of the local environment. Science 2005;308:873–6.

Wilson MA, McNaughton BL. Dynamics of the hippocampal ensemble code for space. Science 1993;261:1055–9.

Wirth S, et al. Single neurons in the monkey hippocampus and learning of new associations. Science 2003;300:1578–81.

Wong RW, Setou M, Teng J, Takei Y, Hirokawa N. Overexpression of motor protein KIF17 enhanced spatial and working memory in transgenic mice. Proc Natl Acad Sci USA 2002;99:14500–5.